Application of Machine Vision in Modeling of Grape Drying Process

N. Behroozi Khazaei[1], T. Tavakoli Hashjin[1*], Hassan Ghassemian[2], M. H. Khoshtaghaza[1], and A. Banakar[1]

ABSTRACT

A method based on Machine Vision System (MVS) is hereby employed to evaluate grape drying through an assessment of the fruit's shrinkage and quality during the dehydration. Experimental data as well as captured images are obtained at an air velocity of 1.4 m s^{-1} and different drying temperatures (50, 60, 70ºC). The results indicated the effect of temperature on the moisture content, shrinkage and color changes. The moisture content along with color changes (ΔE) were modeled and linear regressions applied to correlate the fruit's shrinkage as well as color features to the moisture content. The results obtained, displayed that there existed good linear relationships between the fruit's moisture content, and shrinkage as well as color. The results also revealed that the moisture content *vs*. quality of the grape could be online evaluated through machine vision during the drying process.

Keywords: Grape drying process, Machine vision system, Shrinkage, Quality.

INTRODUCTION

Dried grapes (raisins) from the third biggest utilization way of the grapes, following wine and the use as table grapes. Drying grapes, either through exposure to sunshin, shade drying or artificial drying from some ways of making raisins (Jairaj *et al*., 2009).

Drying grapes through an artificial mechanical hot air dryer is a long time taking process which degrades the quality of the final product. Grape drying process falls within the falling rate period (Esmaiili *et al*., 2007). A prediction of the resulting product's moisture content based on either the temperature and humidity of the outlet air or temperature of the output product was difficult. That was because the outlet air drying parameters and temperature of the output material didn't undergo significant changes ((Margaris and Ghiaus, 2007; Esmaiili *et al*., 2007), therefore it was difficult to predict the moisture content of the resulting material. On the other hand, facilities needed for making measurements had to be of high accuracies which would be expensive.

Nowadays, due to the increasing consumers' demands for healthier grape byproducts of brighter color and also the use of raisins in foods and refreshments, many studies have been carried out on hot air grape drying processes (Pangavhane *et al*., 1999; Karathanos and Belessiotis, 1997; Doymaz and Pala, 2002; Azzouz *et al*., 2002; Ramos *et al*., 2004; Zomorodian and Dadashzadeh, 2009; Esmaiili *et al*., 2007; Ramos *et al*., 2010).

Color is a very important determining factor for representing the dried grape's quality. The color and appearance of the final product more

_____

[1] Department of Agricultural Engineering Machinery, Faculty of Agriculture, Tarbiat Modares University, Tehran, Islamic Republic of Iran.

* Corresponding author; e-mail: ttavakol@modares.ac.ir

[2] Department of Electrical and Computer Engineering, Faculty of Civil Engineering, Trbiat Modares University, Tehran, Islamic Republic of Iran.

than any other parameters were affected by the drying conditions and played the greatest role on the final product's consumer acceptance (Behroozi, 2007).

Therefore, to achieve a high quality product along with the final desired moisture content, online measurement of quality and moisture content as well as a precise controlling of the drying aparatus are essential. This makes the application of innovative technologies as quite indispensable. A few series of modern technologies are nowadays employed for on-line modeling, controlling and optimization of the drying process (Wang *et al.*, 2009; Martynenko, 2006; Romano *et al.*, 2011), Machine Vision (MV) being one of them. Development of machine vision created the opportunity for online monitoring of biomaterial quality (Davies, 2000). Due to the tremendous resolution characteristic of machine vision as regards morphological quantifying (Majumdar and Jayas, 2000, Rashidi *et al.*, 2009) and color (Tao *et al.*, 1995), it was successfully applied in biomaterials' classification. Size and color of undergo appreciable grapes change during drying, and MV is a technology that can measure them throughout the process of grape drying.

Shrinkage during dehydration of fruits and vegetables occurrs when the visco-elastic matrix contracts into the space previously occupied by the water removed from the cells (Aguilera *et al.*, 2003). Since shrinkage modifies the shape and dimension of products, which in turn affects the mass transport phenomena, it is considered as an important consequence of fruit drying (Wang and Brennan, 1995). McMinn and Magee (1997) reported a linear correlation between the shrinkage and moisture content during drying of cylindrical samples of potato tuber in a tunnel dryer. Some researchers applied MV for measuring shrinkage and found a linear relationship between the shrinkage trait and moisture content (Mendiola *et al.*, 2007; Yadollahinia *et al.*, 2008).

Color is an important quality attribute resulting from the interaction between light, the object and the observer. While the kinetics of color change in dried products is least understood, color is still one of the important features in food industry that significantly influences a consumer's purchasing decisions. In a majority of cases, changes in color reflect chemical, biochemical and microbiological reactions (Dafontoura and Marcondes, 2001). A trough understanding of various changes in color can provide an appropriate approach to optimize the drying process and hence minimize the degradation of quality attributes. Several predictive models have been proposed for quality modeling. Empirical models have been employed to predict changes of fruits and vegetables' color during drying. The majority of these works have reported either zero or first order degradation reaction kinetics (Mohammadi *et al.*, 2008; Bahloul *et al.*, 2009).

Fernandez *et al* (2005) presented a method based on computer vision to analyze the effects of drying on shrinkage, color and texture image in apple discs. All the shape related parameters (area, perimeter, Fourier energy, etc.) decreased with drying time. As regards the sample color, lightness (L*) it almost remained constant while the chromatic co-ordinates (a* and b*) increased progressively. Mohebbi *et al.* (2009) estimated shrimp dehydration through an analysis of color change during the drying process as based upon MV.

Martynenko (2006), and Martynenko and Yang (2007) developed an intelligent control system for thermal processing of the natural biomaterials, based on MV. The results revealed the advantage of machine vision in real-time imaging of morphological, color and textureal attributes in a provision of sufficient discriminatory information concerning biomaterial moisture and quality.

However, a gap between image attributes and drying process variables (moisture, quality) appears to be the limiting factor to the use of machine vision in the control of grape drying process. The objective followed in this work is to use machine vision for an online measurement of shrinkage and color changes during grape drying process. The next objective is then to find the relationship

between these parameters and moisture content and quality degradation under different hot air drying temperature conditions. The imaging system was further developed to have pictures taken from the thin layer bed.

MATERIALS AND METHODS

Samples

Seedless Sultana grapes (*Vitis vinifera* L.) from Uremia (Western Azerbaijan Province, Iran) were tested in the experiments. The grapes were randomly selected from the same vine clones. The moisture content of the grapes was determined through the AOAC method (AOAC, 1990). To increase water passage through the waxy skin covering of the berries, the grapes were dipped in two alkaline emulsions of 2.5% K_2CO_3+2% olive oil before the drying operation. Dipping time in the pretreatment solution was about 1 minute at ambient temperature (Pangavhane *et al*., 1999; Doymaz and Mehmet, 2002).

Drying Experiments

A thin layer drying apparatus was employed to dry the grape samples (Figure 1). It controls the drying air temperature as well as velocity through online weighing measurements (digital balance, Sartorius GE812, Germany, with Star to connect software, accuracy of 0.01 g.) during the drying of the samples. The experimental set up is in a way that can generate any desired conditions of the drying air (temperature and velocity). As for the control of heater power for adjusting the air temperature and velocity an SSR relay (Solid State Module, Fotek Co., Taiwan) and an inverter (ENC, 0.4 KW, China) were respectively employed. The sample carrying tray is square shaped with 20 cm dimensions and with a bottom surface square wire mesh of 4 mm. For recording of the samples' weights, the dryer is equipped with a digital balance which weighs within every 5 minute intervals. The whole body of the dryer is thermally
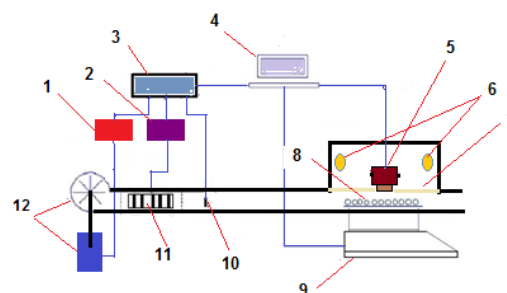
Figure 1. Schematics of the experimental dryer coupled with the image recording system: (1) Inverter; (2) SSR rely; (3) D/A transducer; (4) Computer; (5) Camera; (6) Florescent lamp; (7) Fiber glass; (8) Thin layer grapes; (9) Balance; (10) Temperature sensor; (11) Heater, (12) Fan and electromotor.

insulated with glass wool. The inverter and SSR relay receive signals from computer for adjusting temperature and velocity of the drying air of the dryer.

An analog camera (SCC-101 PA) connected to the computer via a capture card (ACEDVio, Canopus) acts as an image acquisition system. To avoid glare colors, lightening conditions as the main factors are to be attended to (Kopparapu, 2006). To meet the purpose, fiber glass was installed at the front of the lightening source. As 36W florescent tube lamp was made use of to light up the experimental surroundings.

Two programs were prepared in MATLAB software for the drying system. The first adjusted and controlled the drying air's velocity and temperature. It also set the camera to capture images within 20 minute intervals. The second program was made use of in image processing analysis following the completion of any of the experiments.

The drying experiments were conducted at 1.4 m s^{-1} of air velocity and three levels of air temperature (T_1= 50, T_2= 60 and T_3= 70°C) (Pangavhane *et al*., 2000; Yaldiz *et al*., 2001). In each experiment, 300 gr samples of grapes were placed on the tray in a single layer. The experiments were performed in triplicate with the average values being reported. Grapes' moisture content (gr gr^{-1} db) was calculated (from continuous weight measurements) as a

ratio between weight of water (variable) and dry matter weight (constant). The grapes were dried out from an initial moisture content of 2.6±0.25 (db) to the final one of 0.17- 0.18 (db).

Image Analyses

The images were captured in RGB channel (Figure 2-a). Image analysis consisted of smoothing, image segmentation, features extraction, and data analysis. The image process algorithm uses a Gaussian filter for removing the noise of the picture. Image segmentation is designed to separate the grape samples from the background. For the propose, the image of B channel is subtracted from the R channel (Figure 2-b). Then the output image (R-B) is converted into a binary (0, 1) image with Otsu's method for determining threshold and 1 being assigned to the object pixels while 0 is assigned to the background pixels. Erosion and elimination commands were made use of to clear the samples from grape stems (Figure 2-c). The binary image is used for two purposes: (a) estimation of the morphological features (area) and (b) masking on the original color image to extract the color features. Multiplication of the original image on its binary mask enables a conversion of all the background pixels to zero intensity ones (Figure 2-d) (Gonzalez and Woods, 2008)

Image features which are determined as time-dependent variables are further used in data analysis to calculate the physical parameters of drying (moisture content and quality).

Features Extraction

Morphological Features:

Area (A): Number of pixels within the boundary.

Area Ratio (AR), in fact, shows the shrinkage during drying and is calculated through Equation (1):

$$AR = A/A0 \qquad (1)$$

Color Features

Color features are extracted from the R, G and B channels in the RGB color space.

$$RR = R/R_0 \qquad (2)$$

$$RG = G/G_0 \qquad (3)$$

$$RB = B/B_0 \qquad (4)$$

where *RR*, *RG* and *RB* are color ratios, while *R*, *G* and *B* the mean values at time *t*; R_0, G_0 and B_0 are the initial mean values at time *t= 0* in the red, green and blue channels in the RGB color space.

The quality is calculated in the Lab color space. Therefore it is necessary to convert RGB to the Lab color space. RGB values are initially converted into the CIE XYZ system through Equations (5-7):

$$X = k_1 R + k_2 G + k_3 B \qquad (5)$$

$$Y = k_4 R + k_5 G + k_6 B \qquad (6)$$

$$Z = k_7 R + k_8 G + k_9 B \qquad (7)$$

where the *R, G* and *B* are the three pixel grayscale components (Red, Green and

Figure 2. (a) Original picture; (b) Image of R-B; (c) Binary image, (d) Masking original color image.

Blue), *X, Y, Z* the tri-stimulus values in the CIE 1931 system; and k1–k9 standing for the standard coefficients (International Telecommunication Union, 2002). The obtained *X, Y, Z* values are then converted into the CIE L*a*b* values (Equations 8-10).

$$L^* = 116\left(\frac{Y}{Y_n}\right)^{\frac{1}{3}} - 16 \qquad (8)$$

$$a^* = 500\left[\left(\frac{X}{X_n}\right)^{\frac{1}{3}} - \left(\frac{Y}{Y_n}\right)^{\frac{1}{3}}\right] \qquad (9)$$

$$b^* = 500\left[\left(\frac{Y}{Y_n}\right)^{\frac{1}{3}} - \left(\frac{Z}{Z_n}\right)^{\frac{1}{3}}\right] \qquad (10)$$

where *Xn, Yn* and *Zn* (0.95; 1.0; 1.08) represent the *X, Y, Z* values of the European Broadcasting Union with reference white at D65 illumination (Nobbs and Connolly, 2000). Then this color space is used to calculate the total color (Equation 11) (Gorjian *et al.*, 2011):

$$\Delta E = \sqrt{(L^* - L_0)^2 + (a^* - a_0)^2 + (b^* - b_0)^2} \qquad (11)$$

Mathematical Model of Moisture Content and Quality

Two models of moisture content as a function of time are developed on the assumption of the exponential drying model (Diamante and Munro, 1993; Senadeera *et al.*, 2003; Rafiee *et al.*, 2009; Tahmasebi *et al.*, 2011)

$$MR = \frac{M(t) - M_e}{M_0 - M_e} = \exp(-kt) \qquad (12)$$

$$MR = \frac{M(t) - M_e}{M_0 - M_e} = \exp(-kt^N) \qquad (13)$$

Equations (12) and (13) are known to be the Exponential and Page's equation, respectivly. The values of the equilibrium moisture content, M_e, are relatively small as compared with either *M* or M_0. Thus (*M(t)* –

Me)/(M_0-M_e) is simplified to *M/M_0* (Doymaz and Pala, 2002; Kassem *et al* ., 2011). Where M_0 is the initial moisture contents kg kg^{-1} (db), *t* denoting the drying time (h), *k* is the drying rate constant (h^{-1}), *N* product constant, and *MR* standing for the moisture ratio. Kinetics of color changes of fruits and vegetables are generally found to follow zero (Equation 14) and first order (Equation 15) reaction kinetics (Villota and Hawkes, 2007; Devahastin and Niamnuy, 2010):

$$C(t) = C_0 + Kt \qquad (14)$$

$$C(t) = C_0 Exp(Kt) \qquad (15)$$

where *C* is color parameter, C_0 the initial color parameter, *K* standing for color kinetic rate (1 h^{-1}) and *t* for the drying time (h). The temperature dependence of the color kinetic rate and the drying rate constant was explained through Arrhenius equation (Devahastin and Niamnuy, 2010; Sawhney *et al.*, 2009).

$$k \, or \, K = b_0 Exp\left(-\frac{b_1}{T}\right) \qquad (16)$$

where b_0 and b_1 are constants and *T* the absolute air temperature (K). Also the statistical model of the moisture content as a function of the shrinkage and color is developed from the experimental data on the assumption of a linear relationship existing between moisture content, and shrinkage and color:

$$MR = d_1 + d_2\left(\frac{A}{A_0}\right) \qquad (17)$$

$$MR = f_1 + f_2\left(\frac{R}{R_0}\right) \qquad (18)$$

where d_1, d_2, f_1 and f_2 are constants. Experimental data for the different temperatures are fitted to the models and processed through SPSS (version 13.0) software to find the model constants.

RESULTS AND DISCUSSION

The moisture ratio variations and the fitted models *vs.* drying time for the temperatures

of 50, 60 and 70°C have been presented in Figure 3-a. As expected, drying of the grape at higher temperatures resulted in shorter drying times. This indicates that temperature directly affects moisture changes and so the drying time. Similar results have been observed from the grape drying curves (Doymaz and Mehmet, 2000; Esmaiili *et al*., 2007). The drying times of grapes dried at 50, 60 and 70°C air temperature were recorded at 48, 28 and 15 hours past, respectively. These results demonstrate that the drying at 70°C treatment corresponded with drying times of 86.6% shorter than that at 60°C and 220% shorter than that at 50°C. But Doymaz and Mehmet (2002) reported 41, 20.5 and 13.5 hours for drying at 50, 60 and 70°C of air temperature to reach the final desired moisture content of the grapes. Their findings also showed that drying at 70°C took 51 and 179% shorter times of drying than drying at 60 and 50°C. Esmaiili *et al*. (2007) reported 10, 16 and 20 hours for drying times at 70, 60 and 50°C, the difference being due to variations between the thermo-physical properties of the drying air, physical properties of the grape, specifications of the airflow as well as the technical aspects of the dryer employed in each of the studies.

To estimate the moisture content as a function of drying time, the empirical Page and Exponential equations were fitted and the correlation coefficients calculated. The values of R^2 obtained Page equation are higher than those attained from the Exponential one. The R^2 values for Page equation vary between 0.995 and 0.997, and while they vary between 0.985 and 0.995 for the Exponential equation (Table 1). Both equations verify the correlation between the moisture content and

Table 1. Non-linear regression for an estimation of the Exponential and Page models.

	Exponential model		Page's model		
T(°C)	k	R^2	k	N	R^2
50	0.028	0.995	0.022	1.07	0.997
60	0.062	0.985	0.039	1.13	0.995
70	0.118	0.991	0.089	1.17	0.997

drying time. Figure 3-a shows the experimental as well as fitted drying curves. Azzouz *et al*. (2002) and Sawhney *et al*. (2009) reported that Page's equation stands better for a modeling of grape drying process.

As evident from Table 1 the drying rate constant k in Page's equation, increases with increasing air temperature from 0.022 (50°C) to 0.039 (60°C) and to 0.089 h⁻¹ (70°C). The very small value of drying rate constant indicates that the most likely physical mechanism of the grape mass transfer is diffusion. Arrhenius equation was fitted to the drying rate constant with a regression coefficient of 0.952 (Table 3). Similar results were found by Azzouz *et al*. (2002) for the drying of grapes. Also product constant (N) increases with increase in air temperature, but at a low scale (about 4%). In spite of very small variation of the *N* values at different temperatures of the drying air, Sawhney *et al*. (2009) suggested that it was not advisable to use its average figure for all the temperatures and velocities. For a given temperature condition, it is more appropriate to use the velocity average value of *N* at that temperature. But Azzouz *et al*. (2002) reported that the value of *N* is dependent only upon the velocity of the dying air, and on the initial moisture content. Senadeera *et al*. (2003) also concluded that *N* was constant with the drying air temperature when the drying curves related to bean, potato and pea were simulated through the Page model. Hence for very small variation of *N* with temperature it is tempting to ignore these variations and use the average value of *N* (= 1.129). Consequently, the following equation was derived for thin-layer drying of the fruit grape:

$$MR(T,t) = Exp\left(-6.8E8 * Exp\left(-\frac{7.8E3}{T}\right) * t^{1.129}\right)$$
(19)

Figure 3-b presents the area ratio of grapes' changes with temperature during the drying time. It shows that the area ratio decreases with increase in the drying temperature. Ramos *et al*. (2004) reported the same results, namely: a gradual overall shrinkage of grape cells during the drying

process, and an increase in the rate of cellular shrinkage with increase in temperature.

Figure 3-c illustrates a decreasing of the L^* values with drying time. As seen from the figure, L^* values are reduced from 35±1 to around 16±1.5 during hot air drying of the fruit samples. Doymaz and Pala (2002), and Amiri Chayjan *et al.* (2011) reported the L^* values around 18±1.5 for final dried grape at different temperatures. They didn't present any information regarding either the decrease or increase of L^* value during drying time but reminded that with an increase in drying temperature, the L^* value increases. For redness/greenness scale, initial color of samples shows a negative a^* value (about -2), indicating greenness. The final a^* values reached (+1±0.3), indicating redness (Figure 3-d). Therefore, grape sample seems to lose its greenness when dried through hot air. A decreasing in b^* value (Figure 3-e) is also observed during hot air drying. The initial and final b^* values are changed from 7.4 to 2. The color changes may be due to either the non-enzymatic or enzymatic reactions during the drying process (Aguilera *et al.*, 1987). Matteo *et al.* (2000) reported the decrease in L^* value to be very low. Also the a^* and b^* values increased during the drying process. The difference between this paper's results and Matteo *et al.*'s (2000) is due to the condition of treatment solution and also the difference at such initial properties of grape like color and moisture content. Bingol *et al.* (2012) also reported that the L^* and b^* values decreased while a^* value increased during grape drying process under the grape's different pretreatment conditions.

As a whole, the total color changes (ΔE) of the grapes increase during hot air drying with the drying time, ranging from 17 to 15 as air temperature increased from 50 to 70°C, respectively, (Figure 4). Table 3 shows regression analysis of the total color modeling. It is found that the total color changes predicted through zero order
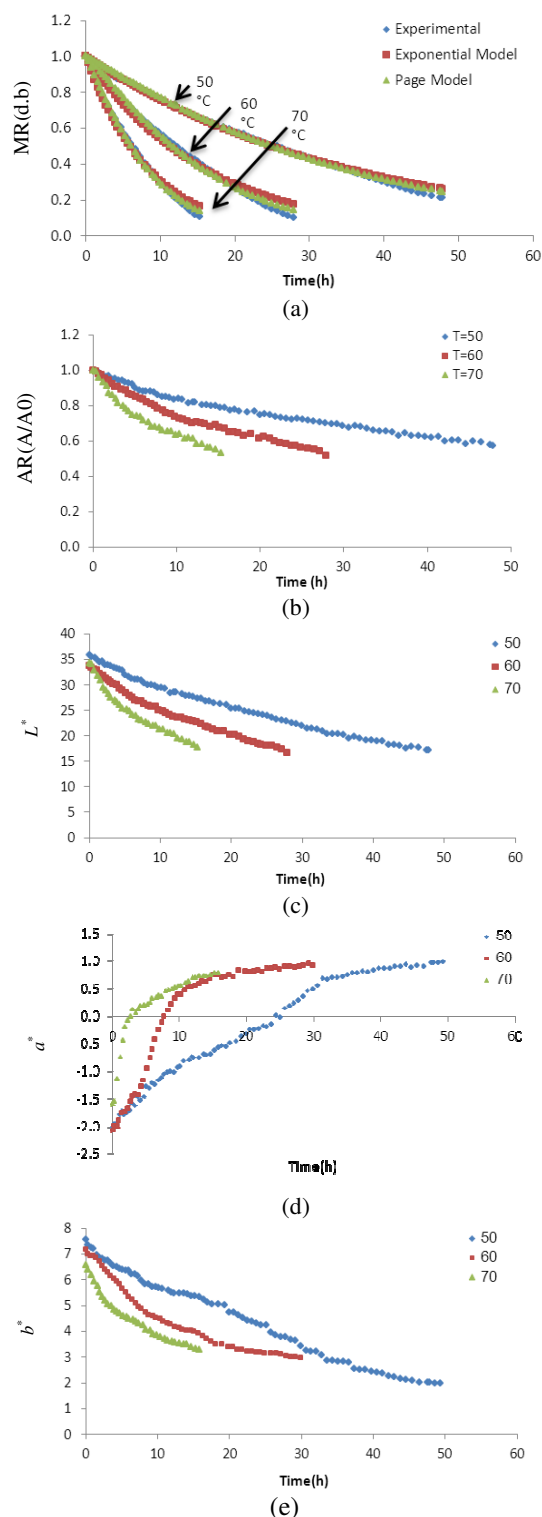
Figure 3. Effect of drying temperature on, moisture ratio (MR), area ratio (AR), and color coordinate values (*L**, *a**, *b**) *vs.* time.
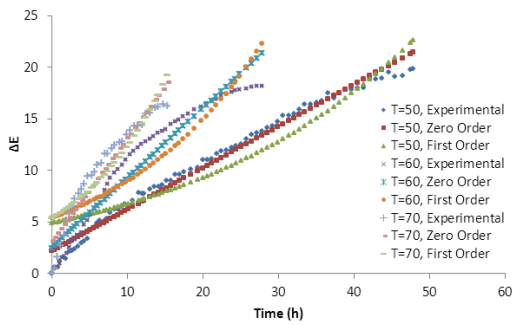
Figure 4. Effect of drying temperature on total color changes (ΔE) *vs.* time.

model were more accurate than the first order model. Figure 4 shows the experimental data and the fitted zero order *vs.* first order models. Mohammadi *et al*. (2008) found similar results for color kinetics modeling of kiwi fruit. The color kinetic rate in the zero order equation increased with increase in drying temperature from 0.403 (50°C) to 0.67 (60°C) and to 1 (70°C) (Table 2). The variations of color kinetic rate with drying temperature were modeled through Arrhenius equation with a regression coefficient of 0.997 (Table 3). The following equation was thus obtained for the color kinetic reaction of grapes during the drying process:

$$\Delta E(T,t) = 2.6 + \left(1.75E6 * Exp\left(-\frac{4.93E3}{T}\right) * t\right)$$
(20)

For the C_0 constant in the color kinetics equation, the mean value obtained from the given figures in Table 2 (C_0= 2.6) was used. Validation of the determined models for prediction of moisture content (Equation 19) and color kinetics (Equation 20) was established by comparing the experimental data, for each drying curve, with the values predicted by these models. The results are plotted in Figure 5. The results show that these equations can predict the moisture content and quality degradation with 0.987 and 0.947 coefficients of determination, respectively. These equations can be used for predicting the moisture content and quality for all temperatures in the range of 50 to 70 °C.

Figure 6 illustrates the variations of *RR, RG*, and *RB* color ratio with time during the drying time. All the color ratios in RGB color space decrease with time and the color variations in the R, G and B channels at the different temperatures are closely similar. For this reason, only the R color ratio is used a prediction of the moisture content. Many a number of researchers have used the Lab color space for a measurement of color kinetics for food during drying process. In addition to the Lab color space, MV creates the opportunity for measuring color changes in the RGB color space throughout the drying process.

Figure 7 shows the relationships between moisture ratio *vs.* area and color ratios in different temperatures media. The statistical model of the moisture ratio as a function of

Table 2. The estimated kinetic parameters and the statistical values of zero *vs.* first-order models for *ΔE*.

	Zero order model			First order model		
T(°C)	*K*	C_0	R^2	*K*	C_0	R^2
50	0.403	2.17	0.981	0.032	4.9	0.892
60	0.67	2.503	0.929	0.051	5.38	0.805
70	1	3.15	0.923	0.084	5.31	0.822

Table 3. Non-linear regression for an estimation of Arrhenius equation *vs.* linear regression for estimating shrinkage and color models.

Arrhenius equation for dying rate constant			Arrhenius equation for color kinetic rate			Shrinkage model			Color model		
b0	b1	R^2	b2	b3	R^2	d1	d2	R^2	f1	f2	R^2
6.8E8	7.81E3	0.988	1.75E6	4.93E3	0.997	1.968	-0.924	0.988	1.427	-0.427	0.982
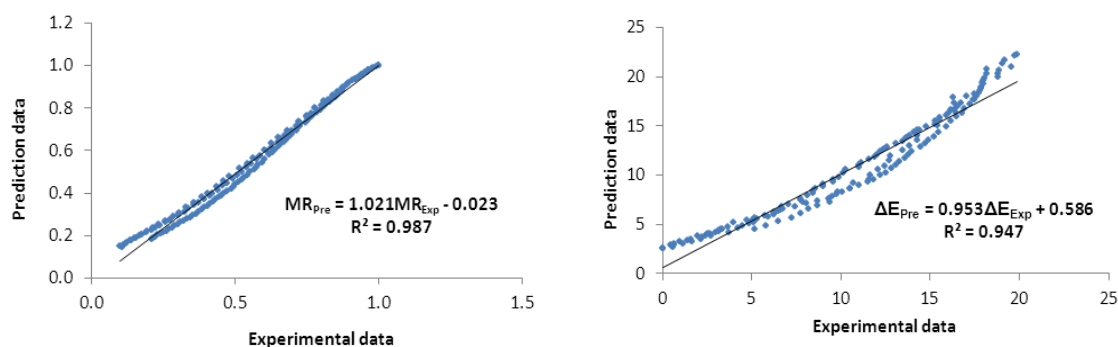
Figure 5. A comparison of experimental data of moisture ratio (MR) and total color changes (ΔE) with the predicted data of (MR) and (ΔE) as by Equations (19) and (20).

the shrinkage and color is reported in Table 3. The coefficients of determination in table 3 show that *MR* is in an acceptable linear relationship with the shrinkage ($R^2= 0.988$) and as well with red color ratio ($R^2= 0.982$). Martynenko (2007) and Yadollahinia *et al*. (2008) reported a similar view of the relationship between shrinkage and moisture content. Ramos *et al*. (2010) and Azzouz *et al*. (2002) have also come across similar concludings for the shrinkage of grapes during the drying process. These results revealed that *MV* can predict the moisture content as based on the shrinkage and color changes throughout a fruit's drying process, and which can be employed in the online control and assessment of the grape moisture content and quality.

CONCLUSIONS

kinetic behavior as regards moisture

content and grape quality throughout the drying process were modeled. These models were applied and tested for an optimization of the drying process. The results indicated that by an evaluation of shrinkage and color through machine vision, the moisture content and quality can be on line predicted during the drying process. Applied machine vision for a control of grape drying process as based upon shrinkage and color was finally found out to be very helpful. Here way *MV* is applied to capture and processes images and then calculates the shrinkage, color ratio and quality of the fruit samples. Later, and through linear relationships between moisture content and either shrinkage or color ratio, the moisture content of the fruit will be predicted. When the moisture content reaches the desired level, the drying process will be terminated and stopped. Step by step quality of the drying grapes can also be monitored throughout the whole drying process.
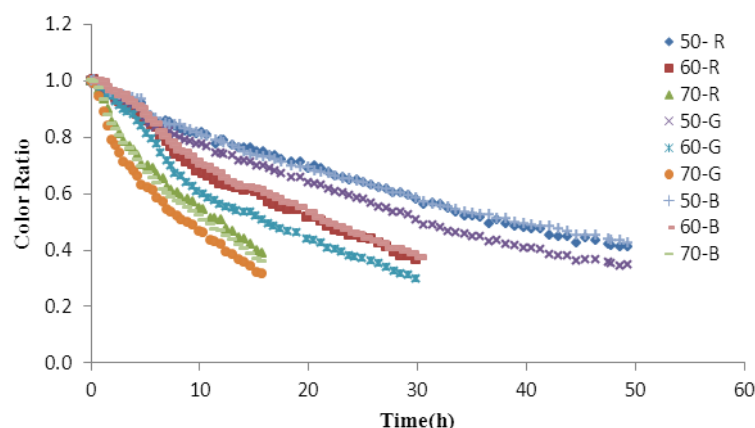
Figure 6. Effect of drying temperature on total color changes (ΔE) *vs.* time.
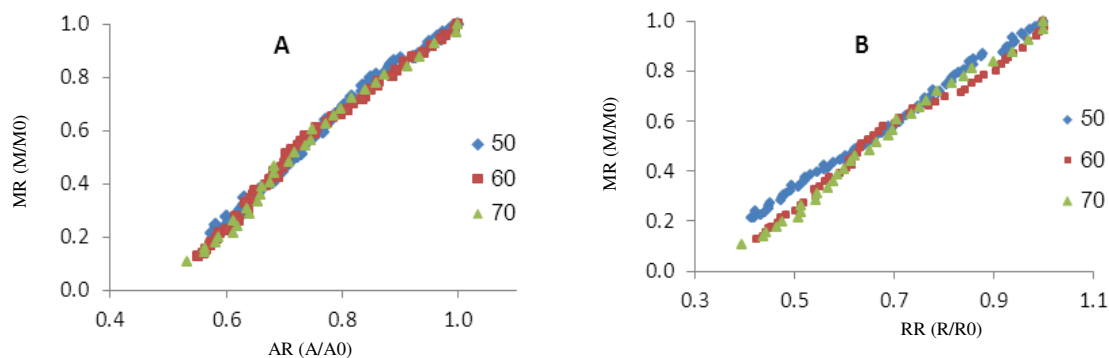
Figure 7. Relationship between moisture ratio (MR) and: (A) Area shrinkage (AR), (B) Red color ratio (RR).

Nomenclature

AR	Area ratio
A_0	Area (number of pixels) at time t_0
A	Area (number of pixels) at time *t*
RR, RG and *RB*	Red, green and blue color ratio, respectively
R, G and *B*	Mean of red, green and blue channel in RGB image at time *t*
R_0, G_0 and B_0	Mean of red, green and blue channel in RGB image at time t_0
MR	Moisture ratio
M_0	Initial moisture content (db)
M_e	Equilibrium moisture content (db)
M(t)	Moisture content (db) at time t
k	Drying rate constant (h^{-1})
N	Product constant
K	Color kinetic rate (h^{-1})
a1, a2, b1, b2	Equation constants.

REFERENCES

1. Aguilera, J. M. 2003. Drying and Dried Products under the Microscope. *Int. J. Food Sci. Tech.,* **9(3):** 137–143.

2. AOAC Report No. 934.06. 1990. *Association of Official Analytical Chemists.* Arlington, VA.

3. Azzouz, S., Guizani, A., Jomaa, W. and Belghith, A. 2002. Moisture Diffusivity and Drying Kinetic Equation of Convective Drying of Grapes. *J. Food Eng.,* **55:** 323–330.

4. Aguilera, J. M., Oppermann, K. and Sanchez, F. 1987. Kinetics of Browning Sultana Grape. *J. Food Sci.,* **52(4):** 993-1025.

5. Amiri Chayjan, R., Peyman, M. H., Esna-Ashari, M. and Salari, K. 2011. Influence of Drying Conditions on Diffusivity, Energy and Color of Seedless Grape after Dipping Process. *AJCS,* **5(1):** 96-103.

6. Behroozi khazaei, N. 2007. Quality Prediction of Raisin Using Artificial Neural Network. MSc. Thesis. Department of Mechanic of Agricultural Machinery, Agricultural Faculty, Tarbiat Modares University, Tehran, Iran.

7. Bahloul, N., Boudhrioua, N., Kouhila, M. and Kechaou, N. 2009. Effect of Convective Solar Drying on Colour, Total Phenols and Radical Scavenging Activity of Olive Leaves (*Olea europaea* L.). *Int. J. Food Sci. Tech.,* **44:** 2561–2567.

8. Bingol, G., Roberts, J. S., Murat, O., Balaban, M. and Devres, Y. O. 2012. Effect of Dipping Temperature and Dipping Time on Drying Rate and Color Change of Grapes. *Dry. Technol.,* **30:** 597-606.

9. Dafontoura, L. and Marcondes, R. J. 2001. *Shape Analysis and Classification: Theory and Practice*. CRC Press, New Jersey, USA, PP. 658.

10. Davies, E. R. 2000. Image Processing for the Food Industry. World Scientific, River Control, Edge, NJ, Singapore, PP. 289.

11. Doymaz, I. and P. Mehmet. 2002. The Effects of Dipping Pretreatments on Air-

drying Rates of the Seedless Grapes. *J. Food Eng.,* **52:** 413-417.

12. Diamante, L. M. and Munro, P. A. 1993. Mathematical Modeling of the Thin Layer Solar Drying of Sweet Potato Slices. *Solar Energy,* **51(4):** 271–276.

13. Esmaiili, M., Rezazadeh, G., Sotudeh-Gharebagh, R., Mousavi, M. A. E. and Rezazadeh, GH. 2007. Influence of Dipping on Thin-layer Drying Characteristics of Seedless Grapes. *Biosys. Engin.,,* **98:** 411–421.

14. Fernandez, L., Castillero, C. and Aguilera, J. M. 2005. An Application of Image Analysis to Dehydration of Apple Discs. *J. Food Eng.,* **67:** 185–193

15. Gonzalez. R. and Woods. R. 2008. *Digital Image Processing.* 3rd Edition, Publisher in Prentice Hall, USA, PP. 976.

16. Gorjian, Sh., Tavakkoli Hashjin,T., Khoshtaghaza, M. H. and Nikbakht, A. M. 2011. Drying Kinetics and Quality of Barberry in a Thin Layer Dryer. *J. Agr. Sci. Tech.,* **13:** 303-314.

17. International Telecommunication Union. 2002. Recommendation ITU-R BT.709 Parameter Values for the HDTV Standards for Production and International Programme Exchange (04/02).

18. Kopparapu, S. K. 2006. Lighting Design for Machine Vision Application. *Image Vision Comput.,* **24:** 720–726.

19. Kassem, A. S., Shokr. A. Z., El-Mahdy. A. R., Aboukarima, A. M. and Hamed, E. Y. 2011. Comparison of Drying Characteristics of 'Thompson' Seedless Grapes Using Combined Microwave Oven and Hot Air Drying. *J. Saudi Soc. Agric. Sci.,* **10:** 33-40.

20. Karathanos, V. T. and Belessiotis, V. G. 1997. Sun and Artificial Air Drying Kinetics of Some Agricultural Products. *J. Food Eng.,* **31:** 35–46.

21. Majumdar, S. and Jayas, D. S. 2000. Classification of Cereal Grains Using Machine Vision. IV. Combined Morphology, Color and Texture Models. *Trans. ASAE,* **43(6):** 1689-1694.

22. Margaris, D. P. and Ghiaus, A. G. 2007. Experimental Study of Hot Air Dehydration of Sultana Grapes. *J. Food Eng.,* 79(4): 1115-1121.

23. Mendiola, R.C., Hernandez, H. S., Perez, J. C., Beltran, L. A., Aparicio, A. J., Fito, P. and Lopez, G. F. 2007. Non-isotropic Shrinkage and Interfaces during Convective Drying of Potato Slabs within the Frame of the Systematic Approach to Food Engineering Systems (SAFES) Methodology. *J. Food Eng.,* **83:** 285–292.

24. Mohammadi, A., Rafiee, R., Emam-Djomeh, Z. and Keyhani, A. 2008. Kinetic Models for Color Changes in Kiwifruit Slices During Hot Air Drying. World Journal of Agricultural Sciences 4 (3): 376-383.

25. Mohebbi, M., Akbarzadeh, M., Shahidia, F., Moussavi, M. and Ghoddusid, H. 2009. Computer vision systems for moisture content estimation in dehydrated shrimp. Comput. Electron. Agric.,69, 128-134.

26. Martynenko, A. I. 2006. Computer-Vision System for Control of Drying Processes. Drying Technology, 24: 879–888

27. Martynenko, A. I., and Yang, S. 2007. An Intelligent Control System for Thermal Processing of Biomaterials. Proceedings of the 2007 IEEE International Conference on Networking, Sensing and Control, London, UK, 15-17 April

28. McMinn, W.A.M., and Magee, T.R.A. 1997. Quality and physical structure of a dehydrated starch-based system. Drying Technology 15 (6), 1961–1971.

29. Nobbs, J. H., & Connolly, C. 2000. Camera-based colour inspection. Sensor Review, 20, 14 – 20.

30. Pahlavanzadeh, H., Basiri, A. and Zarrabi, M. 2001. Determination of parameters and pretreatment solution for grape drying. Drying Technology, 19(1), 217–226

31. Pangavhane, D. R., Sawhney, R. L., and Sarsavadia, P. N. 1999. Effect of various dipping pretreatment on drying kinetics of Thompson seedless grapes. J.Food Eng., 39, 211–216.

32. Pangavhane, D. R., Sawhney, R. L. and Sarsavadia, M. 2000. Drying kinetics studies on single layer Thompson seedless grape under controlled heated air conditions. J Food Process Pres., 24, 335-352

33. Tao, Y., Heineman, P. H., Varghese, Z., Morrow, C. T. and Sommer, H. J. 1995.III, Machine vision for color inspection of potatoes and apples. Transaction of the ASAE, 38 (5), 1555-1561, Oct.

34. Tahmasebi, M., Tavakoli Hashjin, T., Khoshtaghaza, M. H. and Nikbakht A. M. 2011. Evaluation of Thin-Layer Drying Models for Simulation of Drying Kinetics of Quercus (Quercus persica and Quercus libani). J. Agr. Sci. Tech., 13: 155-163.

35. Jairaj, K.S., Singh, S.P. and Srikant K. 2009. A review of solar dryers developed for grape drying. Solar Energy, 83: 1698–1712.

36. Rafiee, Sh., Keyhani, A., Sharifi. M., Jafari, A., Mobli, H., and Tabatabaeefar A. 2009. Thin Layer Drying Properties of Soybean (Viliamz Cultivar). *J. Agric. Sci. Technol.,* **11:** 289-300.

37. Ramos, I. N., Miranda, J. M. R., Brandao, T. R. S. and Silva, C. L. M. 2010. Estimation of Water Diffusivity Parameters on Grape Dynamic Drying. *J. Food Eng.,* **97:** 519–525.

38. Ramos, I.N., Silva, C.L.M., Sereno, A.M., Aguilera, J.M. 2004. Quantification of Microstructural Changes during First Stage Air Drying of Grape Tissue. *J. Food Eng.,* **62(2):** 159–164.

39. Romano, G., Argyropoulos, D., Nagle, M., Khan, M. T. and Müller, J. 2012.Combination of Digital Images and Laser Light to Predict Moisture Content and Color of Bell Pepper Simultaneously during Drying. *J. Food Eng.,* **109**: 438-448.

40. Rashidi, M., Gholami, M. and Abbassi, S. 2009. Cantaloupe Volume Determination through Image Processing. *J. Agr. Sci. Tech.,* **11:** 623-631.

41. Senadeera, W., Bhandari, B. R., Young, G. and Wijesinghe, B. 2003. Influence of Shapes of Selected Vegetable Materials on Drying Kinetics during Fluidized Bed Drying. *J. Food Eng.,* **58(3):** 277–283.

42. Yadollahinia, A., Latifi, A. and Mahdavi, R. 2008. New Methods for Determination of Potato Slice Shrinkage during Drying. *Comput. Electron. Agric.,* **65(2):** 268-284.

43. Yadollahinia, A. and Jahangiri, M. 2009. Shrinkage of Potato Slices during Drying. *J. Food Eng.,* **94:** 52–58.

44. Yaldiz, O., Ertekin, C. and Uzun, H. I. 2001. Mathematical Modeling of Thin Layer Solar Drying of Sultana Grapes. *Energy,* **26:** 457–465.

45. Wang, H. G., Senior, P. R., Mann, R., and Yang, W. Q. 2009. Online Measurement and Control of Solids Moisture in Fluidized Bed Dryers. *Chem. Eng. Sci.,* **64:** 2893-2902.

46. Wang, N. and Brennan, J. G. 1995. Changes in Structure, Density and Porosity of Potato during Dehydration. *J. Food Eng.,* **24:** 61-76.

47. Zomorodian, A. A. and Dadashzadeh, M. 2009. Indirect and Mixed Mode Solar Drying Mathematical Models for Sultana Grape. *J. Agr. Sci. Tech.,* **11:** 391-400.

کاربرد ماشین بینایی در مدلسازی فرایند خشک کردن انگور

ن. بهروزی خزاعی، ت. توکلی هشجین، ح. قاسمیان، م. ه. خوش تقاضا، و ا. بناکار

چکیده

در این مقاله از سیستم ماشین بینایی برای ارزیابی فرایند خشک کردن انگور با اندازه گیری چروکیدگی و کیفیت محصول در طول فرایند خشک کردن استفاده شد. آزمایش ها با سرعت جریان هوای ۱/۴ متر بر ثانیه و دماهای ۵۰، ۶۰ و ۷۰ درجه سیلسیوس انجام گرفت. نتایج نشان داد دما بر روی تغییرات محتوای رطوبتی، چروکیدگی و رنگ در طول فرایند خشک کردن تاثیر دارد. تغییرات محتوای رطوبتی و کیفیت محصول در طول فرایند خشک کردن مدل سازی شد و همچنین از رگرسیون خطی برای مدل سازی تغییرات محتوای رطوبتی با چروکیدگی و رنگ استفاد شد. نتایج نشان داد که یک رابطه خطی مناسب بین محتوای رطوبتی با چروکیدگی و رنگ وجود دارد. همچنین نتایج نشان دهنده آن است که تغییرات محتوای رطوبتی و کیفیت انگور را می توان به کمک ماشین بینایی در طول فرایند خشک کردن به صورت آنلاین اندازه گیری کرد.